EXPERIMENTAL ANALYSIS OF A LIQUID DESICCANT CROSS FLOW PLATE-TYPE DEHUMIDIFIER FOR AIR-CONDITIONING APPLICATIONS

Mustafa Jaradat, Martin Mützel, Lars Schiemann, Roland Heinzen, Klaus Vajen, Ulrike Jordan

Institute for Thermal Engineering, Kassel University, Kurt-Wolters-Str.3, 34125-Kassel, Germany
Phone: + 49 561 804 3890, Fax: + 49 561 804 3993, www.solar.uni-kassel.de, solar@uni-kassel.de

1. Introduction

Liquid desiccant air-conditioning systems remove the latent load directly from the air by absorbing the moisture by a strong solution of liquid desiccant. The main components of an open-loop liquid desiccant air-conditioning system are the absorber (dehumidifier) and the desorber (regenerator) as shown in Figure1.

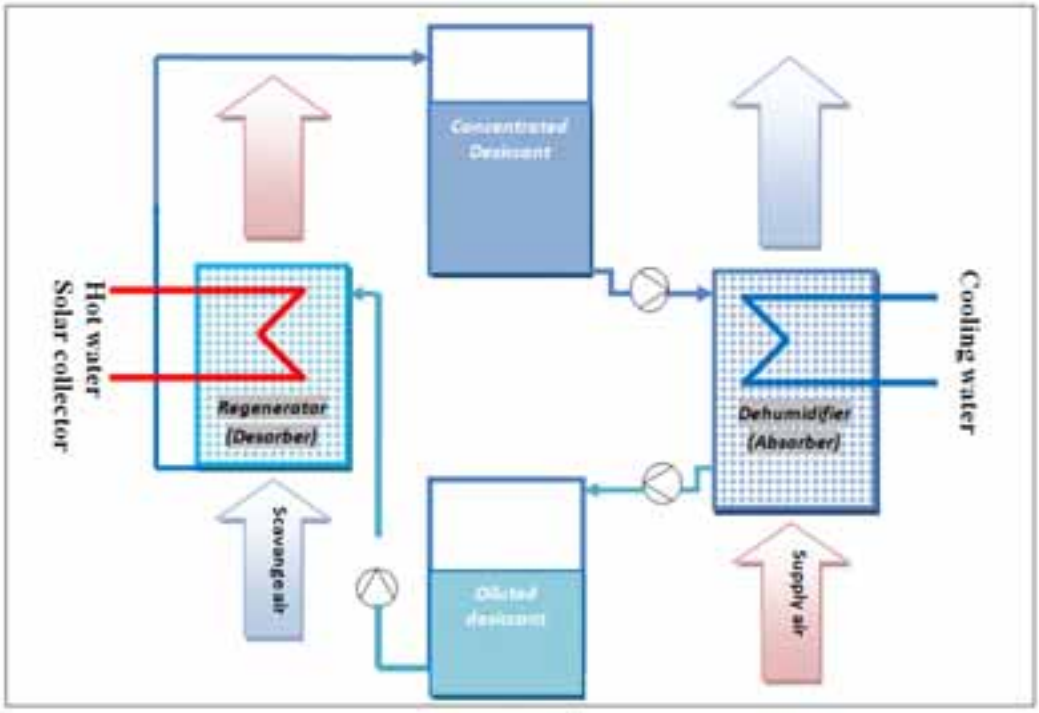

Fig. 1. Schematic diagram of a liquid desiccant air conditioning system

The mass transfer is driven by the difference between the partial pressure of water vapor in the air stream and the vapor pressure associated with the desiccant solution. The vapor pressure above the solution decreases with increasing solution concentration and increases with increasing solution temperature. Therefore, cold and highly concentrated solution provides the best dehumidification while warm and dilute solution provides the best humidification.

In the absorber, moisture absorbed from the conditioned air stream dilutes the desiccant solution by loading the desiccant with water vapor. The solution weakened by absorption of moisture is reconcentrated in the regenerator, where it is heated to elevate its water vapor pressure, the heat drives out the moisture and the strengthened solution is returned to the dehumidifier. A scavenging air stream, usually ambient air, contacts the heated solution in the regenerator. There, water evaporates from the desiccant solution into the air and the solution is reconcentrated.

Liquid desiccant systems overcome the shortcomings of conventional air conditioning systems by decoupling the treatment of latent load from sensible load. The air is dehumidified by being brought into contact with a strong solution of liquid desiccant. When the solution is weakened by absorption of moisture, it is directed to the regenerator where heat drives out the moisture and the strengthened solution is returned to the dehumidifier. To provide sensible cooling in addition to dehumidification, either externally cold water is provided to the dehumidifier, or moisture is added to the air exiting the dehumidifier in order to lower its temperature by adiabatic saturation before it enters the space to be conditioned.

2. Description of the dehumidifier design

Liquid desiccant systems overcome the shortcomings of conventional air conditioning systems by decoupling the treatment of latent load from sensible load. The air is dehumidified by being brought into contact with a strong solution of liquid desiccant. When the solution is weakened by absorption of moisture, it is directed to the regenerator where heat drives out the moisture and the strengthened solution is returned to the dehumidifier. To provide sensible cooling in addition to dehumidification, either externally cold water is provided to the dehumidifier, or moisture is added to the air exiting the dehumidifier in order to lower its temperature by adiabatic saturation before it enters the space to be conditioned.

The prototype consists of a stack of plates, made out of standard twin-wall polycarbonate plates. One of the important aspects in this heat and mass exchanger requires the separation between the driving force medium (cooling water) and liquid desiccant solution. This feature was realized by the use of double panels commercially called twin-wall plates. Those plates have internal square channels through which the driving cooling or heating water passes. The heat is transferred through the wall between the water and the liquid desiccant. This prototype represents a plate type heat and mass exchanger in which heat is transferred between the desiccant and water; the water and desiccant media are separated by the twin-wall to prevent mixing.

The polycarbonate extruded sheets has the dimensions of 600x600 mm^2 and a thickness of 6 mm. The network structure of the channels ensures even distribution of the circulated water with a sufficient strength.

Six plates are installed in parallel; the distance between two adjacent plates is the width of the air passage. The air passage between two adjacent plates in the current prototype is 5 mm, this distance representing the polycarbonate spacer thickness. Each plate has 105 internal passages with a square cross section of 5x5 mm^2.

The prototype contains an upper and a lower water-feeder box. Each water feed-box consists of four equal chambers separated by baffles, Fig. 2. Cooling water passes through the internal passages of the polycarbonate twin-wall plates in a three-loop serpentine path. It will enter the first chamber from a primary opening in the upper wall of the chamber, and it collides with a perforated spreading surface that faces the internal twin-wall passages. The spreading surface will direct the water equally to the internal channels.

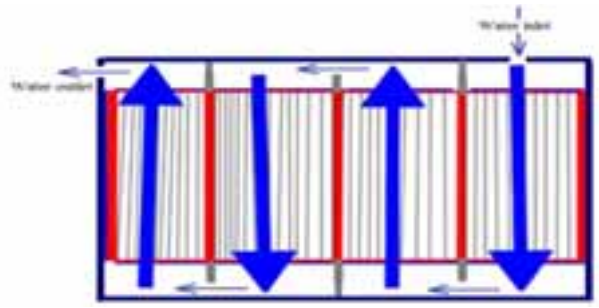

Fig.2. Cooling water flow patterns, 3-loop serpentine path

Heat transfer between the water and the liquid desiccant is in parallel flow configuration in the internal passages connected to the first and the third water champers, and in a counter flow configuration in the internal passages connected to the second and forth water chambers, Fig.3. Counter flow achieved in the second and forth chambers results in a greater effective temperature difference.

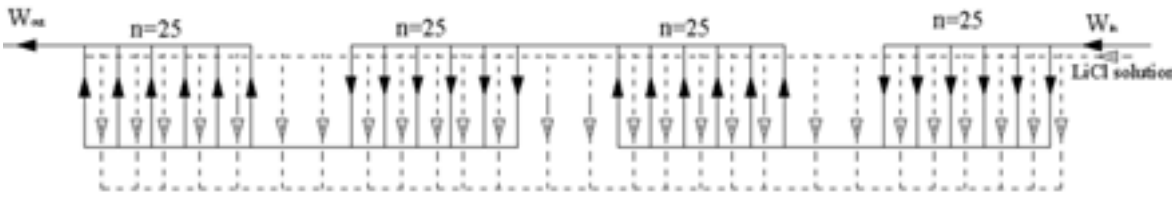

Fig.3. Water-desiccant flow pattern, solid lines represent the water flow and dashed lines represent the desiccant flow, n represents the number of internal cooling water passages

The plates are covered with a promising fleece fiber in order to increase the exposure time of the desiccant on the plates and thereby enhance the desired mass transfer. Also, the diffusion of the desiccant through the textile fibers prevents the desiccant from reuniting to larger runnels due to its high cohesion. The fleece was tested regarding the absorption capacity and the diffusion behavior of the desiccant solution [1].

The liquid desiccant distributor in this design uses a plurality of parallel Poly-methyl methacrylate (PMMA) tubes to horizontally distribute the liquid desiccant over the wick attached to the polycarbonate twin-wall plates. Seven (PMMA) parallel tubes extend outwardly from openings in the lower edge of one of the sides of the liquid desiccant feed box and are closed from the free end. Standard plugs were used to close the perforated pipes from the free end. The outer pipes (the 1st and the 7th) were perforated only from the inner side facing the textile since they are feeding one face only, Figure 4 shows the perforated pipes and how they penetrate the twin-wall plates. The tubes penetrate the polycarbonate twin-wall plates horizontally and deliver the desiccant solution over the coated plates at a number of equally spaced-apart locations (discharge-holes). The discharge holes are preferably formed on the plexiglass tubes by using a CNC machine to make the fine drip points with high precision. The size and number of the discharge holes are selected to provide the desired liquid flow. Likewise, the distance between the discharge-holes is selected to meet the desired liquid desiccant flow rate with the maximum even distribution.

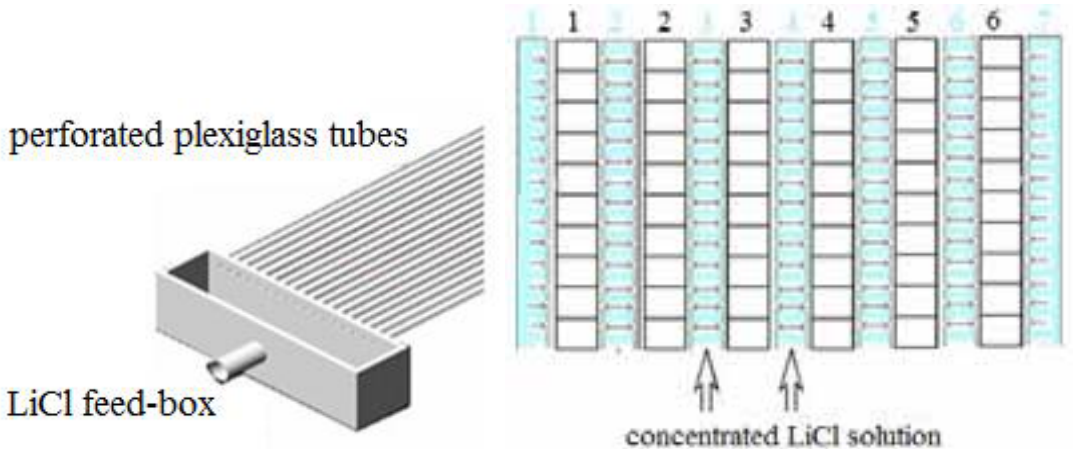

Fig.4. Schematic diagram of the liquid desiccant distribution through perforated (PMMA) pipes. 1-6 represent the PC twin-wall plates and 1-7 represent the perforated plexiglass pipes

3. Instrumentation and experimental setup

3.1. Air channel system

Mass flow and temperature for all of the flow streams as well as water mass fraction in the desiccant and air flow streams were applied in the test-rig. For clarity, each flow circuit will be presented separately in the following.

The desired air flow rate was established with the help of a centrifugal fan. The air is directed by means of a set of valves provided the option of adjusting the direction of the air stream into one of the vortex sensors that were used to measure the air flow rate. The air channel system is applied with two vortexes type OPTISWIRL 4070 DN 100 and DN 150. The first vortex sensor (OPTISWIRL 4070 DN 100) is used for low air flow rates up to 1000 m^3/h.

After passing through the flow meter, the air was directed to an air heating and an air cooling devices as well as a steam generator. The electric air heater, P=20 kW, is controlled by an electronic temperature controller. The air heater is used with PID temperature controller to heat the air to the needed set value. The air could be heated up to 55 °C according to the needed air conditions at the prototype entrance.

Depending on the desired conditions, air can be cooled and/or dehumidified by using an air handling unit. The air handling unit can provide cooling and/or dehumidification of the air according to the needed conditions at the heat and mass exchanger inlet. Chilled water from the laboratory channel is pumped to coils

located in the air handling unit to cool and dehumidify the air stream. The needed air temperature and/or relative humidity for each experiment is controlled by modulating the chilled water flow rate through the air handling unit coils.

In addition the air channel network is equipped with a steam generator device in order to humidify the air according to the required set-value. The steam generator produces non-pressurized steam using heating elements immersed in the water contained in an internal cylinder. The cylinder capacity for the steam generator used is 10 l. The maximum capacity of the humidifier is 10 kg/h. The steam produced is applied to the air channel system isothermally without increasing the inside air temperature.

Relative humidity and temperature are continually monitored by using humidity and temperature transmitters (HygroFlex). The 3-wire humidity temperature transmitter uses chilled mirror and optoelectronic mechanism to detect condensation on the mirror surface. Two HygroFlex sensors were applied in the middle of the round-to-rectangle ducts (at the inlet and outlet) and they positioned deeply in the center of the air flow streams. The air duct system is shown in Figure 5.

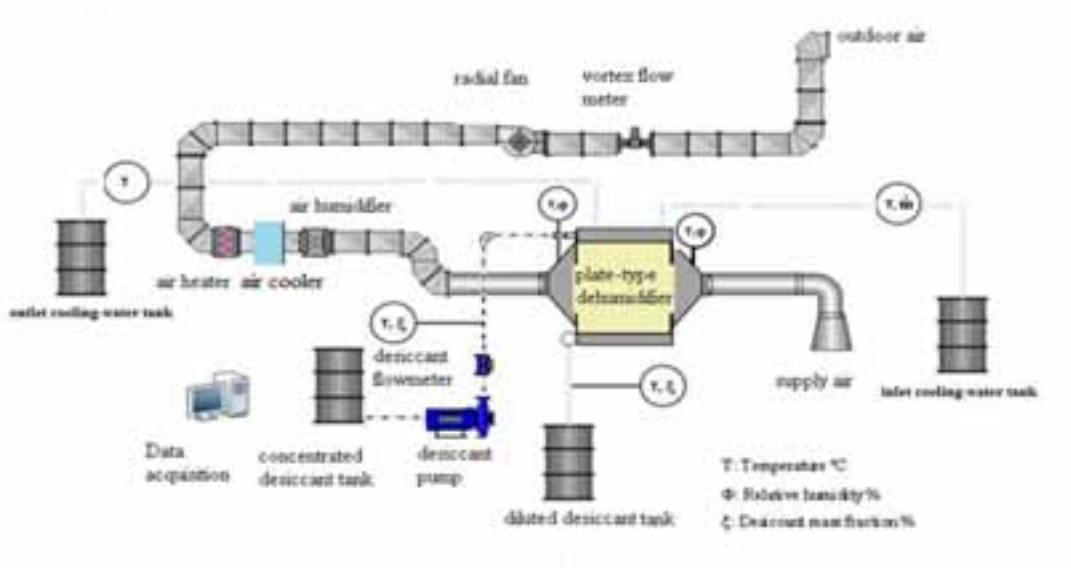

Fig.5. Air duct work with instrumentation

3.2. Desiccant hydraulic system

The liquid desiccant flow circuit is shown in Figure 6. The desiccant circuit consists of two desiccant storage tanks made out of plastic.

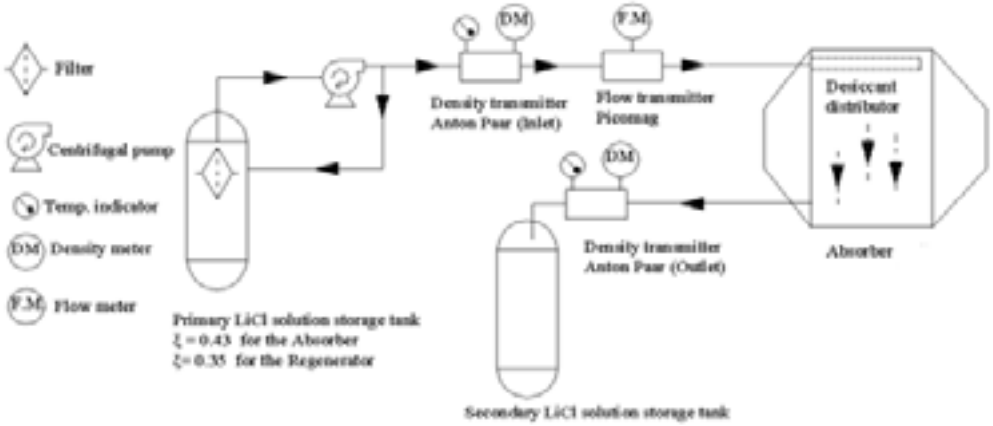

Fig.6. Schematic diagram of the LiCl-solution hydraulic circuit

The desiccant solution was withdrawn from the upper surface of the primary tank with the help of a positive displacement pump. A floater was used to keep the desiccant suction from the surface level so that the flow

rate will not be affected with the head loss during the experiment. A T-valve was connected at the pump outlet port in order to divide the outlet desiccant stream into two streams; one stream is returned back to the primary desiccant tank in order to keep the desiccant homogeneity, and the second stream is directed to the heat and mass exchanger.
A thin plastic sheet made out of polycarbonate was installed directly on the surface of the LiCl solution stored to prevent greater contact of the solution with the air inside the primary tank. A filter with a pore size of 300 μm was installed in the recirculation line to keep the solution clean in order to prevent clogging of the small holes in the desiccant manifold.

The density and the temperature of the LiCl solution discharged from the primary tank to the heat and mass exchanger was continually monitored while passing through a density meter. The density transmitter used in the desiccant circuit was L-Dens 323 from the company Anton Paar.

The flow rate of the strong LiCl solution is continually monitored by using a magneto-inductive flow meter. The desiccant flow meter used in the current desiccant circuit was from the company Endress+hauser.

The LiCl solution left the magneto inductive flow meter entered the desiccant distributor and then throttled over the textile attached over the twin-wall plates. The desiccant is trickles down by gravity and left the prototype. The density and the temperature of the desiccant that left the prototype were continually monitored by passing through the density transmitter (L-Dens 323).

The pipes used for desiccant circulation through the desiccant circuit were made out of polyurethane (ϕ out=12 mm). In order to minimize heat losses, the connections were made as short as possible and the pipes were insulated with tubular type insulation with a slit down the length made out of polyethylene foam (K = 0.42 W/m.K) with a thickness of 50 mm.

3.3. Water hydraulic system

Figure 7 shows the water flow circuit. The circuit consists of two water tanks, the primary tank was insulated with a synthetic rubber insulator (Armaflex, K = 0.033 W/m.K) with a thickness of 25 mm. The water circulated from the primary water tank to the heat and mass exchanger via insulated polyurethane pipes. The water flow rate was continually monitored using a magneto-inductive flow meter. The water inlet and outlet temperatures were continually monitored by using two PT100 sensors. The accuracy for the PT100 sensors were ±0.1 K.

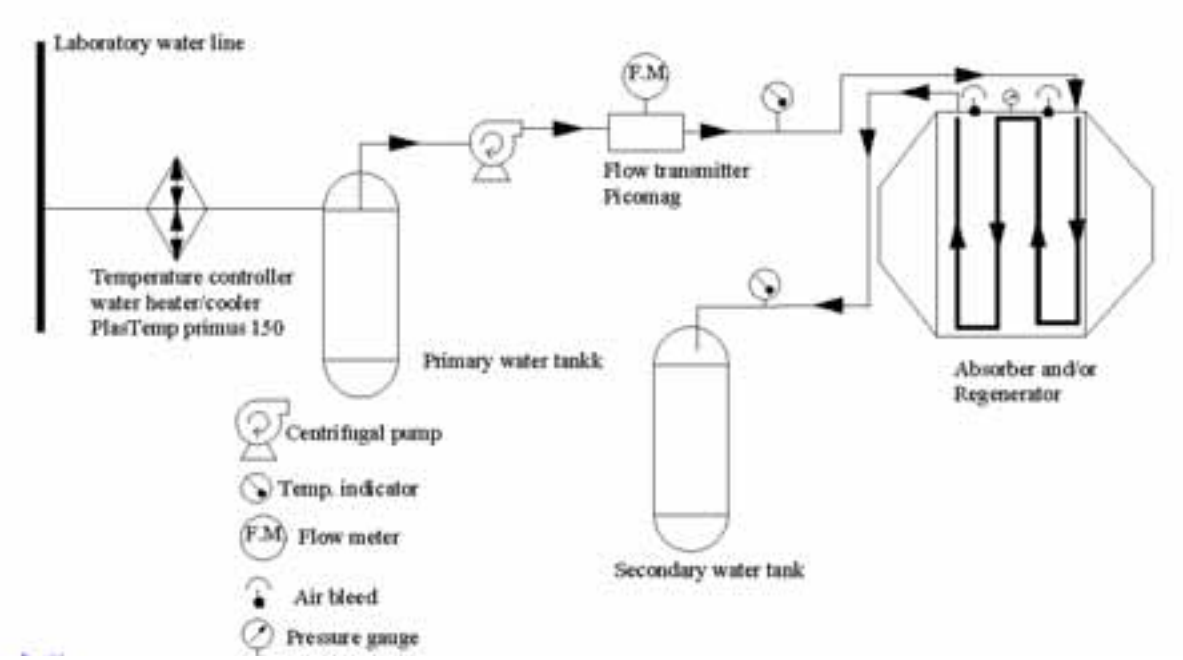

Fig.7. Schematic diagram of the cooling-water hydraulic circuit

The signals from the whole instruments were sent to a data acquisition system LAB/MSR manager was used. The data were saved to an Excel file with a time step of 10 seconds. Figure 8 shows an overall view of the whole system.

Fig.8. Liquid desiccant dehumidifier test-rig

3.4. Experimental setup

Experiments were conducted with the following parameter ranges: fixed air mean flow rate of about 105 g/s, air inlet temperature of 24.5–28.1 °C, air humidity ratio of 12–15.3 g/kg, desiccant flow rate of 2.5–8.5 g /s and water mean flow rate of 19-100 g/s. The air inlet conditions were chosen to comply with one of the test conditions set by ARI Standard 940 (ARI, 1998). Table 1 summarizes the inlet and outlet conditions of all circulated fluids; air, desiccant and water accompanied with the sensors accuracy.

Tab. 1: Inlet and outlet conditions of the circulated fluids; T (temperature), Φ (relative humidity), ρ (desiccant density) and ṁ (mass flow rate)

	$\overline{T}_{a,in}$ °C ±0.3K	$T_{a,out}$ °C ±0.3K	$\overline{\phi}_{a,in}$ % ±1%	$\phi_{a,out}$ % ±1%	$\overline{\dot{m}}_a$ kg/h ±1%	$\overline{T}_{des.,in}$ °C ±0.1K	$\overline{T}_{des.,out}$ °C ±0.1K	$\rho_{des,in}$ g/cm^3 ±0.001	$\rho_{des,out}$ g/cm^3 ±0.001	$\overline{\dot{m}}_{des.}$ kg/h ±0.5%	$\overline{T}_{w.,in}$ °C ±0.1K	$\overline{T}_{w.,out}$ °C ±0.1k	$\overline{\dot{m}}_w$ kg/h ±0.5%
1	27.3	28.5	64.5	45.1	374.9	27.1	32	1.2822	1.2390	13.08	18.2	28.5	70.5
2	27.3	26.8	67.1	49.4	361	28.2	31.4	1.2818	1.2438	15.07	18	25.8	133.2
3	27	25.8	67.9	51.4	375.2	28.7	30.9	1.2815	1.2468	15.51	18.2	24.8	242.7
4	28.1	24.9	59.4	48.9	373.2	27.6	28.9	1.2819	1.2438	13.84	18.2	22.5	357.6
5	28	26.4	61.5	51.1	372.1	27.4	30.3	1.2820	1.2464	15.51	18.2	25	176.1

The experiment runtime was 60 to 75 minutes started when the inlet conditions at the heat and mass exchanger reaches quasi steady state conditions. The aim of the experiments was to study the effect of the cooling water and liquid desiccant flow rates on the air outlet-conditions; temperature and relative humidity.

4. Results and Discussion

The results of the supply air non-adiabatic dehumidification show a consistent reduction in the relative humidity, a consistent reduction in the humidity ratio, and a reduction in the air temperature. In the experimental runs the change in the relative humidity ranges between 8% to 27% points, the change in the absolute humidity ranges between 3.5 to 4.6 g/kg, and the maximum reduction in the air temperature was 3.6 K, depending on the operation conditions of the affecting parameters; water and desiccant flow rate, air inlet temperature and relative humidity. Figure 9 shows the experiment (Tab.1, no. 4), a reduction of about 19% points in the relative humidity and a reduction in the air temperature of about 3.2 K.

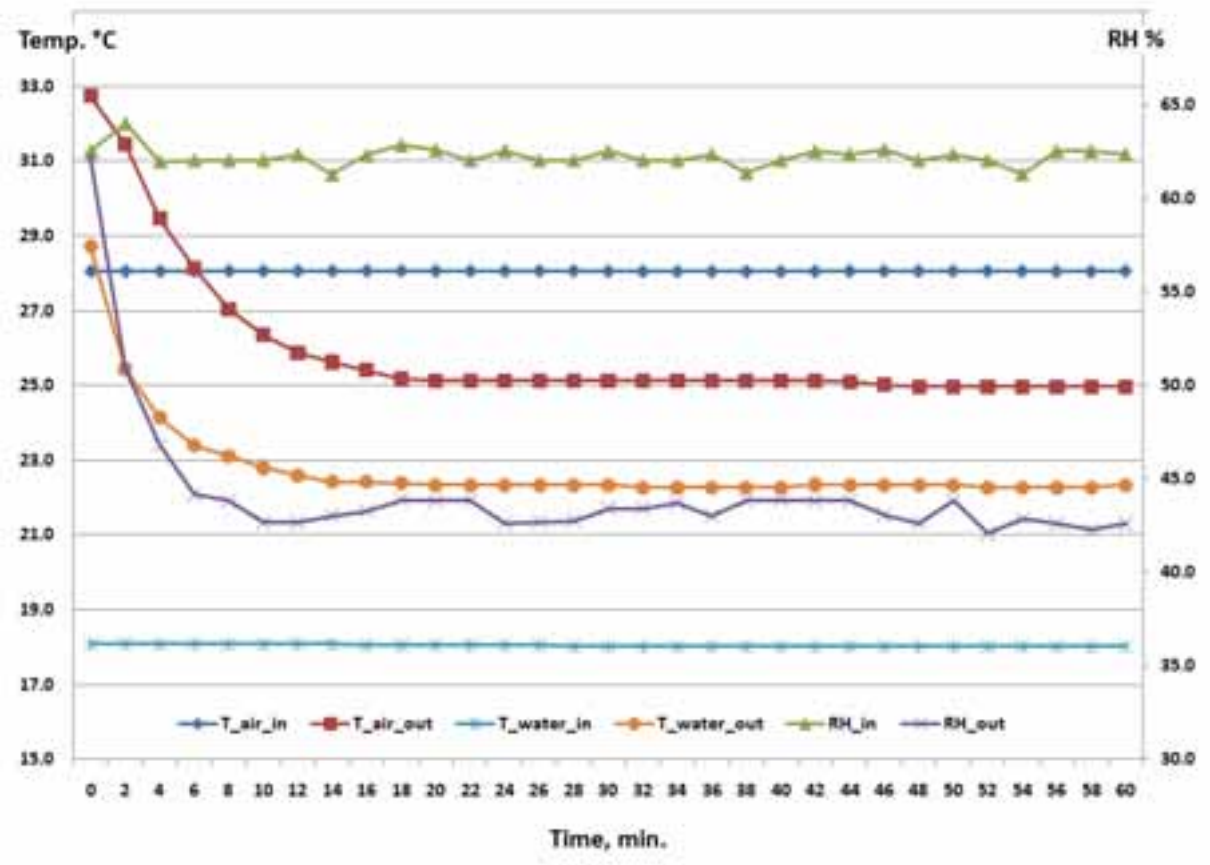

Fig. 9: The interaction between the inlet parameters in one of the experimental runs; $\dot{m}_a$=373.2 kg/h, $\dot{m}_{des.}$=13.84 kg/h, $\dot{m}_{coolingwater}$=357.6 kg/h.

One of the major aspects of this study was to investigate the air outlet conditions on the psychrometric chart with human thermal comfort zones. ASHRAE Standard 55 specifies summer and winter comfort zones appropriate for clothing insulation levels of 0.078 and 0.14 W/m^{2}K, respectively [2]. Figure 10 shows the air inlet and outlet state conditions for the experiment shown above. It is clearly shown in Fig.10 that the air outlet condition is located in the area that represents the interaction between the summer and winter comfort zones.

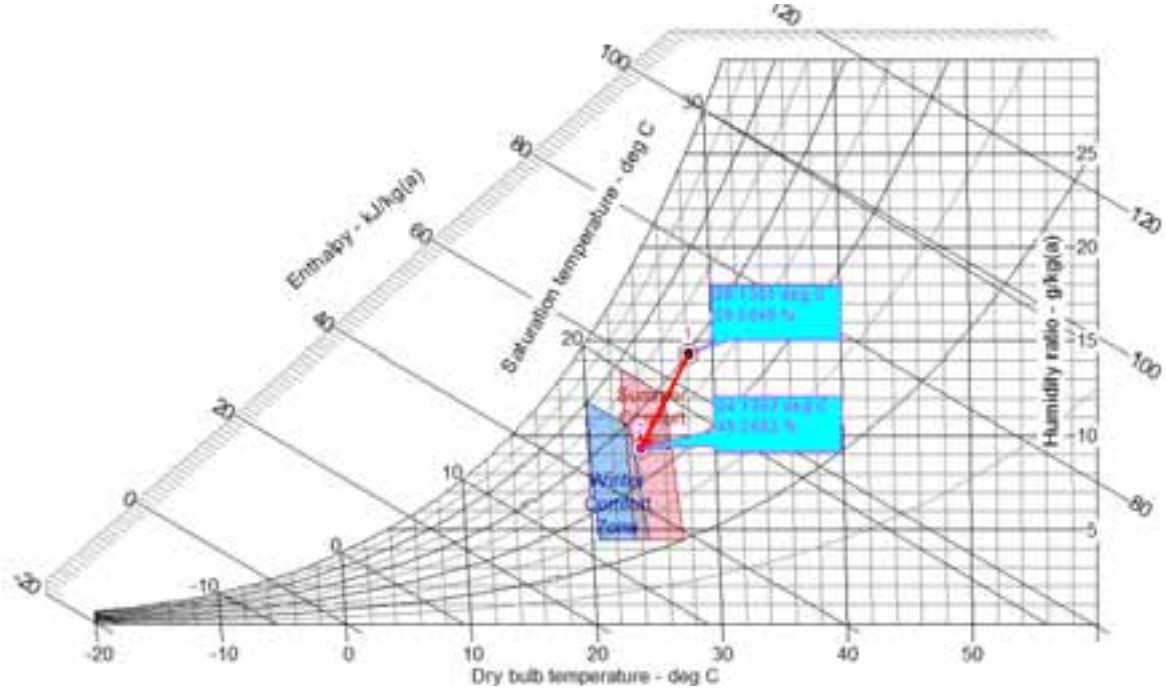

Fig.10: Representation of the 6th experimental run on the psychrometric chart together with the thermal human comfort zones, $T_{db,air,in}$=28.1 ºC, $\omega_{air,in.}$=14.188 g/kg, $T_{des.,in}$=27.6 ºC, $T_{cooling\text{-}water,in}$=18.2 ºC, $\dot{m}_{air}$=373.2 kg/h, $\dot{m}_{des.}$=13.8 kg/h, $\dot{m}_{water}$=357.6 kg/h

The mass transfer performance of the dehumidifier was evaluated in terms of the moisture removal rate and the dehumidifier effectiveness. The moisture removal rate, $\dot{m}_v$, was calculated by Eq. 1 [3]. The dehumidifier effectiveness, ε, is the ratio of the humidity ratio difference of the air passing through the dehumidifier to its difference under ideal conditions, as shown in Eq. 2.

$$\dot{m}_v = \dot{m}_a \cdot (\omega_{a,in} - \omega_{a,out}) \qquad \text{Eq.1}$$

$$\varepsilon = \frac{\omega_{a,in} - \omega_{a,out}}{\omega_{a,in} - \omega_e} \qquad \text{Eq.2}$$

Where, ω_e is the saturation humidity ratio of air at equilibrium with the desiccant solution at the desiccant inlet-temperature. And it is defined as

$$\omega_e = 0.6198 \cdot \frac{P_s}{P_a - P_s} \qquad \text{Eq.3}$$

and, P_s is the saturation pressure in (Pa)and is calculated by Eq. 4

$$P_s(T) = 3 \cdot 10^{-9} \cdot T_{des.,in}^5 - 4 \cdot 10^{-7} . T_{des.,in}^4 + 3 \cdot 10^{-5} \cdot T_{des.,in}^3 + 2 \cdot 10^{-4} \cdot T_{des.,in}^2 - 0.0126 \cdot T_{des.,in} + 0.3 \qquad \text{Eq.4}$$

The dimensionless quantity κ is used to analyze the mass and energy balance between air and desiccant solution. Theoretically, the water vapor absorbed from the air stream should be equal to the water added to the desiccant solution.

$$\dot{m}_a \cdot \Delta\omega = \dot{m}_s . \Delta X \qquad \text{Eq.5}$$

where, X is the water content in the desiccant solution, given by Eq. 6

$$X = \frac{1-\xi}{\xi} \qquad \text{Eq. 6}$$

Reforming Eq.5

$$\kappa_{mass\ balance} = \frac{\dot{m}_a \cdot \Delta\omega}{\dot{m}_S \cdot \Delta X} \qquad \text{Eq. 7}$$

The same procedure was followed to obtain a dimensionless quantity for the energy balance between the process air, desiccant solution and cooling water.

$$\sum \dot{Q}_{system} = \dot{Q}_{air} + \dot{Q}_{sol} + \dot{Q}_{cooling\ water} = 0 \qquad \text{Eq. 8}$$

Rearranging Eq. 8, the enthalpy balance for the circulated fluids was calculated using Eq. 9.

$$\kappa_{energy\ balance} = \frac{\dot{Q}_{air}}{\dot{Q}_{LiCl,sol.} + \dot{Q}_{cooling\ water}} \qquad \text{Eq. 9}$$

The air to desiccant mass ratio (A/D) is given by Eq.10, and the air to cooling water mass ratio (A/W) is given by Eq.11.

$$\frac{A}{D} = \frac{\dot{m}_a}{\dot{m}_{des.}} \qquad \text{Eq.10}$$

$$\frac{A}{W} = \frac{\dot{m}_a}{\dot{m}_{cooling-water}} \qquad \text{Eq.11}$$

Table 2 summarized the moisture removal rate, $\dot{m}_v$, from the air stream to the concentrated LiCl solution, the dehumidifier effectiveness, ε, mass energy balance, $\kappa_{mass\text{-}balance}$, and energy mass balance, $\kappa_{energy\text{-}balance}$.

Tab. 2: Summary of the experimental runs results regarding the moisture removal rate, dehumidifier effectiveness, air to desiccant mass ratio (A/D), air to cooling water mass ratio (A/W) and mass & energy balance.

	$\omega_{air,in}$ [g/kg]	$\omega_{air,out}$ [g/kg]	$\bar{\xi}_{des,in}$	$\xi_{des,out}$	$\bar{\dot{m}}_v$ [g/s]	ε [1]	A/D	A/W	Mass balance κ	Energy balance κ
1	14.72	10.97	0.4405	0.386	0.39	0.33	28.7	5.3	0.76	0.96
2	15.32	10.88	0.44	0.392	0.45	0.38	24.0	2.7	0.87	0.94
3	15.23	10.67	0.44	0.396	0.48	0.40	24.2	1.5	0.99	0.71
4	14.19	9.60	0.44	0.391	0.48	0.42	27.0	1.0	0.98	0.85
5	14.62	10.99	0.44	0.395	0.37	0.32	24.0	2.1	0.77	0.75

The optimal value of κ is equal to unity and any deviation from unity (κ≠1) represents deterioration in dehumidification. The results show a deviation from unity that could be a result of sensors accuracy and measurement errors.

The moisture removal rate, $\dot{m}_v$, the dehumidifier effectiveness, ε, and air outlet temperature, $T_{a,out}$, were studied as a function of cooling water flow rate, $\dot{m}_{cooling\text{-}water}$. Figure 11 shows the results for the tests 1, 2, 3 as set I and the tests 4, 5 as set II. All the inlet parameters were kept nearly constant while varying the cooling water flow rate. The air-to-cooling water mass flow rate for the 1st, 2nd and 3rd runs were 5:1, 2.7:1 and 1.5:1, respectively. And for the 4th and the 5th experiments were 1:1 and 2:1, respectively. Fig. 11 shows that the moisture removal rate and the dehumidifier effectiveness are strongly increased by increasing the cooling water flow rate, and that increasing the water flow rate caused a sharp decrease in the air outlet temperature until a certain limit. An air-to-cooling water mass ratio of about 3:1 results in an isothermal dehumidification for an A/D of 24:1 and cooling water inlet temperature of 18 ºC. The experiments showed that an A/W of 1:1 results in an outlet air temperature that lies inside the thermal summer comfort zone.

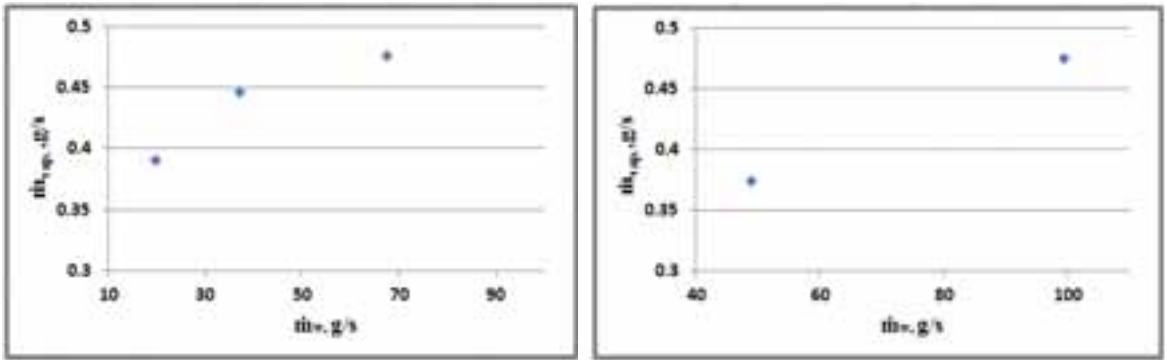

Moisture removal rate versus. the cooling-water flow rate

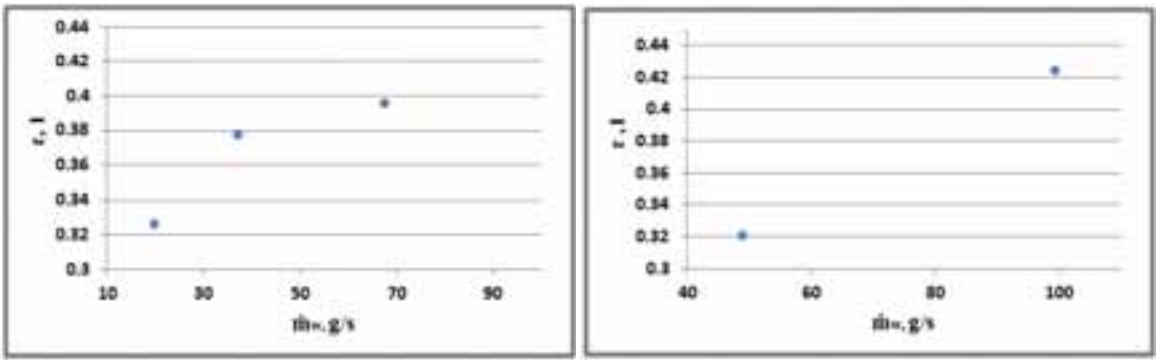

Humidifier effectivness versus the cooling water flow rate

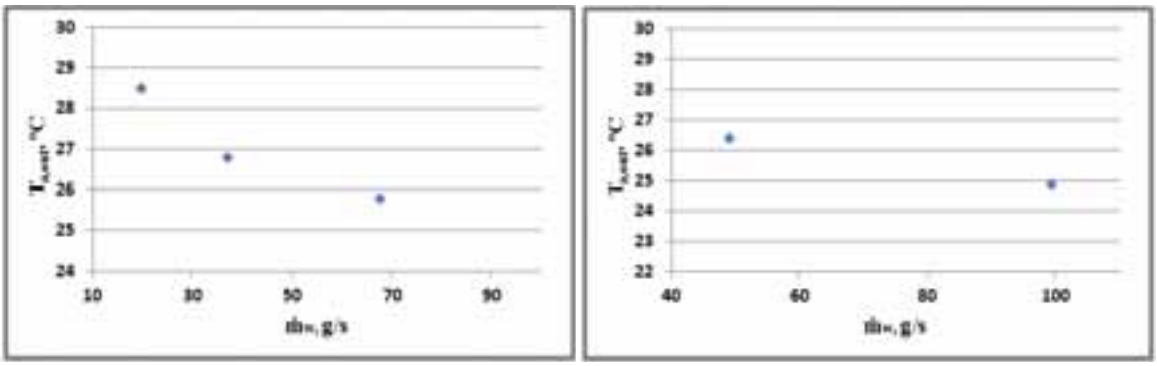

Air outlet temp. versus the cooling water flow rate

Fig. 11: moisture removal rate, dehumidifier effectiveness and air dry-bulb outlet temperature as a function of the cooling water mass flow rate, for experiments. 1, 2 & 3 (left) and experiments 4 & 5 (right)

5. Conclusion

The desiccant dehumidification technology is budding as an alternative to conventional vapor compression systems for space air cooling and conditioning. Desiccant based systems are cost effective because of their use of low grade thermal energy or waste energy to accomplish the same effect for removal of moisture from the air.

The moisture removal rate and dehumidifier effectiveness were adopted as the dehumidifier performance indices. The effects of the dehumidifier inlet parameters, including desiccant and water flow rates, air inlet temperature and humidity ratio were investigated. The air outlet temperature and humidity ratio was studied as a function of cooling water flow rate. The results showed a consistent reduction in the air humidity ratio and temperature that matches the summer comfort zone on the psychrometric chart

The experimental results of supply air dehumidification and cooling showed an effective air

dehumidification and cooling on the thermal comfort zone on the psychrometric chart. The reduction in the supply air humidity ratio ($\Delta\omega$) could reach 4.6 g/kg and a reduction in the supply air temperature of 3.6 ºC.

The paper experimentally studied the heat and mass transfer between three circulated fluids; air, liquid desiccant and cooling water. The moisture removal rate, humidifier effectiveness and supply air outlet temperature were studied as a function of different ranges of cooling water and LiCl flow rates. The mass and energy balance analysis showed promising results.

6. References

[1] Mustafa Jaradat et al." A Novel Generator Design for a Liquid Desiccant Air Conditioning System", EuroSun 2008 Conference, Lisbon (PO), 07.10 - 10.10.2008.

[2] ASHRAE Handbook of Fundamentals, 2001

[3] Lowenstein A., Slayzak S., Kozubal E., A Zero Carryover Liquid Desiccant Air Conditioner for Solar Applications, ASME/Solar06, Denver (US).